

REPORT DOCUMENTATION PAGE

Form Approved
OMB No. 0704-0188

Public reporting burden for this collection of information is estimated to average 1 hour per response, including the time for reviewing instructions, searching existing data sources, gathering and maintaining the data needed, and completing and reviewing this collection of information. Send comments regarding this burden estimate or any other aspect of this collection of information, including suggestions for reducing this burden to Department of Defense, Washington Headquarters Services, Directorate for Information Operations and Reports (0704-0188), 1215 Jefferson Davis Highway, Suite 1204, Arlington, VA 22202-4302. Respondents should be aware that notwithstanding any other provision of law, no person shall be subject to any penalty for failing to comply with a collection of information if it does not display a currently valid OMB control number. PLEASE DO NOT RETURN YOUR FORM TO THE ABOVE ADDRESS.

1. REPORT DATE (DD-MM-YYYY)

4/27/2012

2. REPORT TYPE

Final Technical Report

3. DATES COVERED (From - To)

12/15/2009 - 12/14/2011

4. TITLE AND SUBTITLE

Nanotailored Carbon Fibers

5a. CONTRACT NUMBER

FA9550-10-C-0030

5b. GRANT NUMBER

5c. PROGRAM ELEMENT NUMBER

6. AUTHOR(S)

Dr. Han Gi Chae

5d. PROJECT NUMBER

5e. TASK NUMBER

5f. WORK UNIT NUMBER

7. PERFORMING ORGANIZATION NAME(S) AND ADDRESS(ES)

Nano Engineered Materials Corporation
2250 Abby Lane, Atlanta GA 30345

8. PERFORMING ORGANIZATION REPORT NUMBER

9. SPONSORING / MONITORING AGENCY NAME(S) AND ADDRESS(ES)

Air Force Office of Scientific Research
Dr. Joycelyn Harrison
875 North Randolph Street
Suite 325, Room 3112
Arlington, VA 22203

10. SPONSOR/MONITOR'S ACRONYM(S)

AFOSR

11. SPONSOR/MONITOR'S REPORT NUMBER(S)

12. DISTRIBUTION / AVAILABILITY STATEMENT

This technical report is approved public release with unlimited distribution.

13. SUPPLEMENTARY NOTES

20120504077

14. ABSTRACT

Various spinning trials of polyacrylonitrile (PAN) and PAN/carbon nanotube (CNT) fibers were conducted using single- and bi-component spinning to obtain precursor fiber for carbonization. Materials parameters, such as homo- vs co-polymer, as well as different molecular weight polymers were investigated. In order to obtain better precursor fiber with circular crosssectional shape, gelation bath composition and bath temperature were varied in the spinning process. The precursor fiber containing 0.5 to 1 wt% CNT exhibited tensile strength in the range of 0.6 to 1 GPa and tensile modulus in the range of 16 to 28 GPa. The PAN/CNT precursor fibers were subsequently stabilized and carbonized in the batch process by varying stabilization conditions such as tension, temperature, and residence time. The effective carbon fiber diameter from core precursor fiber was in the range of 3.5 – 4 μ m. The highest average tensile strength and modulus were 5.5 GPa and 362 GPa while the maximum properties for the individual filaments were up to 6.8 GPa and 389 GPa, respectively. This study proves that PAN/CNT technology can be used to process carbon fibers with a tensile strength approaching 7 GPa and tensile modulus approaching 400 GPa at a relatively low carbonization temperature of 1300 degree C.

15. SUBJECT TERMS

STTR report

16. SECURITY CLASSIFICATION OF:

a. REPORT

U

b. ABSTRACT

U

c. THIS PAGE

U

17. LIMITATION OF ABSTRACT

UU

18. NUMBER OF PAGES

14

19a. NAME OF RESPONSIBLE PERSON

Han Gi Chae

19b. TELEPHONE NUMBER (include area code)

404-234-3507

STTR Phase II Final Technical Report

Title: Nanotailored Carbon Fibers

Submitted to: Dr. Joycelyn Harrison, AFOSR/NA

PI: Dr. Han Gi Chae, Nano Engineered Materials Corp.

Table of Contents

1. Abstract.....	1
2. Introduction.....	1
3. Spinning dope preparation	1
4. Precursor fiber preparation.....	3
5. Stabilization and Carbonization of various precursor fibers.....	14
6. Summary and key-outcomes	28

1. Abstract

Various spinning trials of polyacrylonitrile (PAN) and PAN/carbon nanotube (CNT) fibers were conducted using single- and bi-component spinning to obtain precursor fiber for carbonization. Materials parameters, such as homo- vs co-polymer, as well as different molecular weight polymers were investigated. In order to obtain better precursor fiber with circular cross-sectional shape, gelation bath composition and bath temperature were varied in the spinning process. The precursor fiber containing 0.5 to 1 wt% CNT exhibited tensile strength in the range of 0.6 to 1 GPa and tensile modulus in the range of 16 to 28 GPa. The PAN/CNT precursor fibers were subsequently stabilized and carbonized in the batch process by varying stabilization conditions such as tension, temperature, and residence time. The effective carbon fiber diameter from core precursor fiber was in the range of 3.5 – 4 μm . The highest average tensile strength and modulus were 5.5 GPa and 362 GPa while the maximum properties for the individual filaments were up to 6.8 GPa and 389 GPa, respectively. This study proves that PAN/CNT technology can be used to process carbon fibers with a tensile strength approaching 7 GPa and tensile modulus approaching 400 GPa at a relatively low carbonization temperature of 1300 °C.

2. Introduction

PAN is currently the predominant precursor for structural carbon fibers. Pitch-based carbon fibers can have very high tensile modulus with high electrical and thermal conductivity. However, PAN-based carbon fibers have higher tensile and compressive strength. Nonetheless, the tensile strength of current state-of-the-art carbon fiber is only a small fraction of the theoretical strength of the carbon-carbon bond. In order to further enhance the strength and modulus of PAN based carbon fibers, a small amount of CNTs can be used to reinforce PAN precursor fibers. Addition of CNTs induces the graphitic structure in the vicinity of CNTs. In addition, higher strength carbon fibers can be processed by decreasing the fiber diameter. In this STTR phase II program, we use CNTs to reinforce PAN precursor fiber and also utilize bi-component spinning along with gel spinning, to obtain small diameter fibers. Various processing parameters during precursor spinning, stabilization, and carbonization have been carefully studied and optimized.

3. Spinning dope preparation

Various polymers have been used for spinning dope preparation to investigate the effect of polymer type on the resulting carbon fiber. As listed in Table 1, polyacrylonitrile (PAN), poly(acrylonitrile-co-methacrylic acid) (PAN-co-MAA), and poly(acrylonitrile-co-itaconic acid) (PAN-co-IA) polymers with different molecular weights were used. Polymers were obtained from Japan Exlan. As-received polymers were dried in vacuum oven at 100 °C for 2 days under continuous vacuum. Methacrylic acid and itaconic acid content was 4 and 2 wt%, respectively. High purity carbon nanotube (lot no. XO122UA, catalytic impurity - 1 wt%, CCNI, Houston, TX) was used, and CNT content was varied from 0.5 to 1 wt% with respect to polymer. Based on high resolution TEM study, this batch of CNT contains double-, triple-, and few-wall CNT. We also used high purity single wall carbon nanotube (lot no. SPO300, catalytic impurity - 2 wt%, CCNI). Dimethylformamide (DMF) or dimethylacetamide (DMAc) were used as solvent. For the sacrificial component of bi-component spinning (sheath-core or sea-islands geometry), poly(methyl methacrylate) (PMMA) with weight average molecular weight of about 350,000 g/mol was used. The solid concentration for PMMA solution was 30 g/100 mL.

Table 1. List of polymers used for spinning dope preparation.

Polymer ID	Polymer type	Co-monomer content	Viscosity average molecular weight (g/mol)*
P1	PAN homo-polymer	-	250,000
P2	PAN homo-polymer	-	500,000
P3	PAN homo-polymer	-	700,000
P4	PAN-co-MAA**	4 wt%	240,000
P5	PAN-co-MAA**	4 wt%	470,000
P6	PAN-co-MAA**	4 wt%	513,000
P7	PAN-co-MAA**	4 wt%	750,000
P8	PAN-co-IA**	2 wt%	520,000

* Viscosity average molecular weight was provided by manufacturer (Japan Exlan)

** MA and IA stand for methacrylic acid and itaconic acid, respectively.

For spinning dope preparation, we tried to use different methods to achieve homogeneous solution as follows. It should be noted that obtaining homogeneous solution is very important to achieve fiber evenness and consistent fiber properties along the fiber axis.

- **Solution preparation method 1**

The selected polymer was dissolved in distilled solvent at a desired solid concentration. The solid concentration was varied for different molecular weight polymer. CNTs were separately dispersed in solvent at a concentration of 40 mg/L using 24 hr bath sonication (Branson 3510R-MT, 100W, 42 KHz) at room temperature. The sonicated CNT/solvent dispersion was added to polymer solution and the excess amount of solvent was removed by vacuum distillation at a bath temperature of 90 °C, while stirring, to obtain the desired solution concentration. The addition of CNT dispersion and removal of excess solvent was iterated until the desired CNT concentration (0.5 – 1 wt% with respect to polymer) was achieved.

- **Solution preparation method 2**

The half amount of the selected polymer was dissolved in distilled solvent. CNT dispersion procedure was same as described in method 1. After completion of concentrating CNT, we prepared PAN solution separately using the remaining half of the polymer and mix with PAN/CNT solution. The excess amount of solvent was removed to achieve the desired solid concentration. By method 2, one can minimize the molecular weight reduction caused by long time stirring at high temperature. The typical time to prepare about 200 mL (1 wt% CNT composite solution) was about a week. However, it can be noted from the fiber spinning section that the fibers spun from this solution preparation method was not as good as the fiber prepared using method 1 (section 4.6). The resulting carbon fiber properties based on solution preparation method 2 were also poor (Table 18 and Table 19 in section 5.2)

The detailed conditions for each spinning trial are shown in following section (precursor fiber preparation).

4. Precursor fiber preparation

4.1 Single component fiber spinning – effect of spin draw ratio on the properties of precursor fiber

In order to investigate the effect of spin drawing on the resulting precursor fiber properties, various spin draw ratios were adopted for this spinning trial. Various processing conditions and fiber properties are listed in Table 2. As can be seen, hot draw ratio decreased as the spin draw ratio increased. However, the total draw ratio for SCF3 becomes much higher than the other fibers, resulting in smaller diameter and better mechanical property fiber.

Table 2. Various processing conditions and properties of single component precursor fibers.

	SCF1	SCF1	SCF3
Polymer/solvent/concentration	P4 / DMAc / 14.5g/dL		
CNT (concentration)	XO122UA (1 wt%)		
Solution prep. method	Method 1		
Gelation bath temperature	-50 °C		
Spin draw ratio	3	5	10
Hot draw ratio*	11	8.2	6.4
Total draw ratio	33	41	64
Effective fiber diameter (μm)	14.5	13.5	10.1
Tensile strength (GPa)**	0.72 ± 0.08	0.76 ± 0.08	0.86 ± 0.07
Tensile modulus (GPa)**	17.3 ± 1.8	18.5 ± 1.2	21.6 ± 1.5
Strain to failure (%)**	8.6 ± 0.8	8.5 ± 0.7	7.6 ± 0.6

*Hot drawing conducted using glycerol bath at 170 °C. Bath length was about 15 cm, and the resident time for all the fibers was maintained at about 0.3 s by keeping the constant take-up speed at 30 m/min.

** Tensile testing conducted using gauge length of 25.4 mm and cross-head speed of 1%/s.

Figure 1 shows scanning electron microscope (SEM) image. Fiber cross section is kidney-bean shape. Figure 2 is Raman spectra at different orientation angles, and normalized Raman G-band intensity as a function of polarization angle with the fiber axis for SCF3. It can be noted that CNTs are well oriented along the fiber axis (Herman's orientation factor for CNT = 0.92).

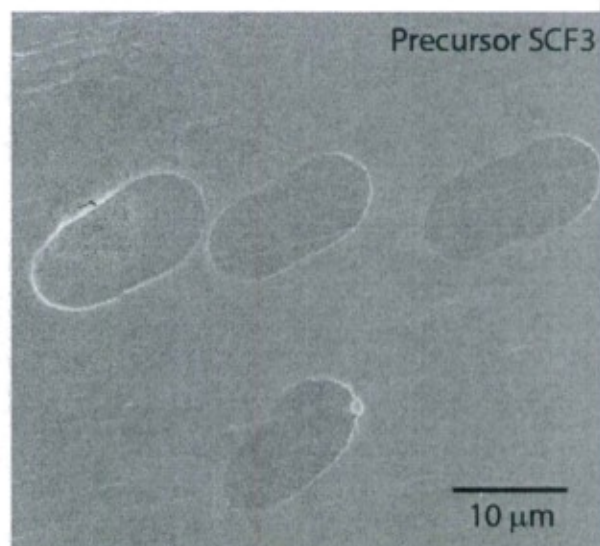


Figure 1. SEM image of cross-sections (SCF3).

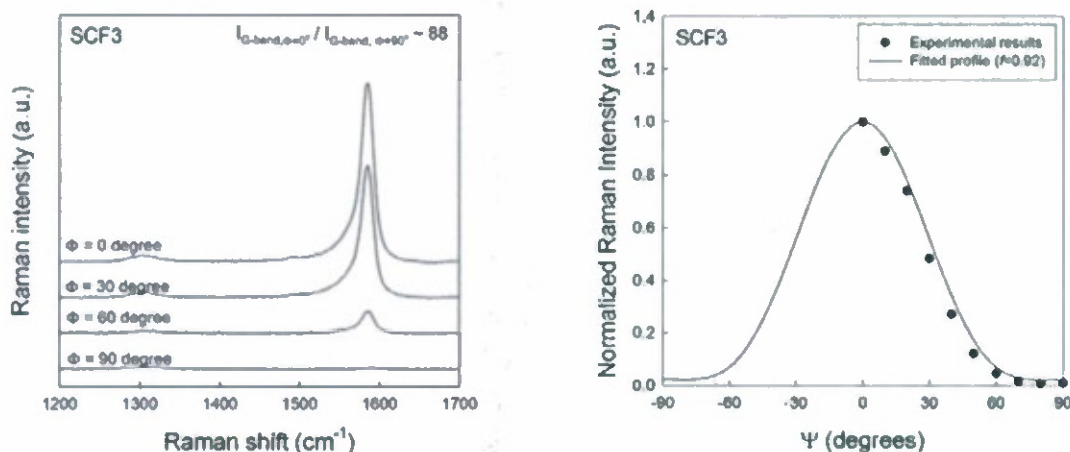


Figure 2. Top: SEM image of fiber cross-sections, Bottom left: Raman spectra showing orientational angular dependence, Bottom right: Raman G-band intensity as a function of orientation angle to calculate orientation factor ($f=0.92$) for SCF3.

4.2 Bi-component (sea-islands) fiber spinning – effect of cold drawing on the properties of precursor fiber

Sea-islands bi-component fiber was spun and drawn using 37 islands geometry. In this spinning trial, we adopted two-stage drawing condition after spinning as shown in Table 3. For tensile testing, sea component (PMMA) was removed by soaking the fiber in nitromethane for about 10 min. It can be noted that cold drawing step improved precursor fiber properties as compared to the fiber drawn directly at high temperature. In addition, island fibers exhibited improved mechanical properties at a relatively low draw ratio as compared to the single component fibers. It should be also noted that tensile modulus of BCFi2 fiber is about 10% higher than that of SCF3, indicating that cold drawing can be very effective to align the molecules along the fiber axis. Figure 3 shows SEM cross-sectional image and Raman spectra as a function of orientation angle for BCFi2. As compared to single components fibers, cross-sectional shape of islands fibers is irregular.

Table 3. Processing conditions and properties of bi-component (sea-islands) precursor fibers.

	BCFi1	BCFi2
Polymer/solvent/concentration	P4 / DMAc / 14.5g/dL	
CNT (concentration)	XO122UA (1 wt%)	
Solution prep. method	Method 1	
Gelation bath temperature	-50 °C	
Spin draw ratio	3	3
Cold draw ratio	N/A	1.4
Hot draw ratio*	8.4	7.6
Total draw ratio	25.2	31.9
Effective fiber diameter (μm)	1.86	1.67
Tensile strength (GPa)**	0.70 ± 0.08	0.85 ± 0.07
Tensile modulus (GPa)**	21.0 ± 1.5	24.5 ± 1.8
Strain to failure (%)**	6.1 ± 0.5	6.7 ± 0.7

*,** Hot drawing and testing conditions were same as for the single component fiber in Table 2.

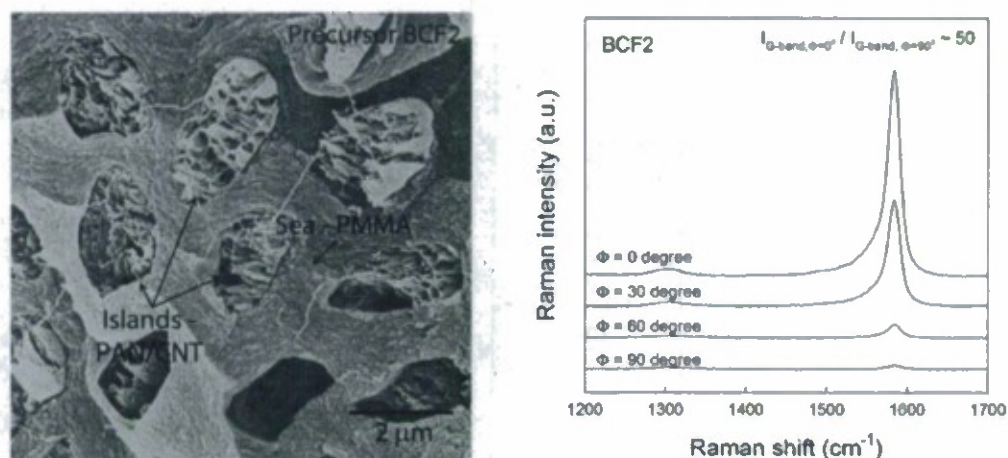


Figure 3. Left: SEM cross-sectional image of BCFi2 and right: Raman spectra showing angular dependence. G-band intensity ratio (parallel to perpendicular) was about 50.

4.3 Single component fiber spinning – effect of gelation bath composition to obtain circular precursor fiber

It is important to obtain circular fiber for carbonization. During spinning, as-spun fiber is going through gelation (or coagulation) bath where the solid fiber is formed. It is important to balance the solvent/non-solvent exchange rate to obtain circular fiber. In this spinning trial, we investigated the effect of gelation bath composition (solvent/non-solvent mixture). Various processing conditions and resulting fiber properties are listed in Table 4.

100% methanol gelation bath led to the highest drawability and tensile properties of the resulting precursor fiber. It can be also noted that the processing stability (drawability) and tensile properties decreased by increasing content of DMAc in gelation bath. However, SEM cross-sectional images (Figure 4) show that one can obtain fairly circular cross-sectional fiber at 40% DMAc content in gelation bath. This

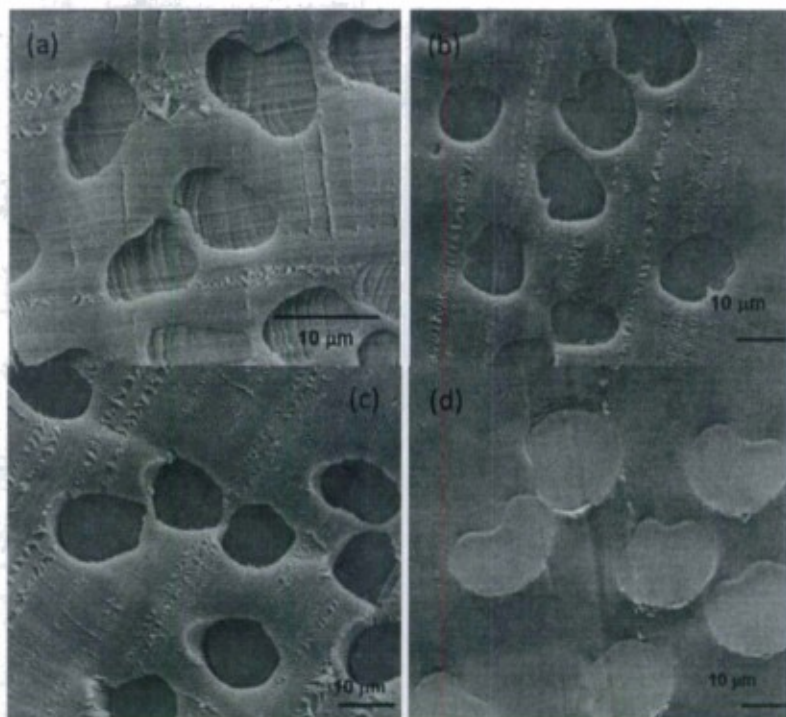


Figure 4. SEM cross-sectional images of PAN precursor fibers processed using various gelation bath compositions. Methanol/DMAc – (a) 100/0, (b) 80/20, (c) 60/40, and (d) 40/60.

may be attributed to the slow solvent-nonsolvent exchange rate in the gelation bath. In addition, fiber processed using 100% methanol gelation bath possesses higher degree of crystallinity as compared to the other fibers (Table 4 and Figure 5).

Table 4. Processing conditions and properties of single component precursor fibers processed using varying gelation bath conditions.

	Gelation bath composition (methanol/DMAc)			
	SCF4 (100/0)	SCF5 (80/20)	SCF6 (60/40)	SCF7 (40/60)
Polymer/solvent/concentration	P3 / DMAc / 7.5g/dL			
CNT (concentration)	CNTs were not used in these trials			
Solution prep. method	Method 1 without CNT			
Gelation bath temperature	-50 °C			
Spin draw ratio	1	1	1	1
Cold draw ratio*	1.55	1.55	1.55	1.23
Hot draw ratio*	8.6	7.6	8.1	5.2
Total draw ratio	13.3	11.8	12.6	6.4
Effective fiber diameter (μm)	10.4	12.8	11.3	16.6
Tensile strength (GPa)**	1.4 ± 0.1	0.8 ± 0.1	0.9 ± 0.1	0.6 ± 0.1
Tensile modulus (GPa)**	24.1 ± 2.1	19.9 ± 2.3	21.9 ± 1.8	17.9 ± 1.5
Strain to failure (%)**	8.0 ± 0.6	6.2 ± 0.6	7.1 ± 1.1	7.6 ± 0.5
Crystallinity (%)***	61	50	54	48
Crystal size (nm)***	13.7	11.0	13.4	12.2
f_{PAN} ***	0.91	0.90	0.90	0.87

* Cold and hot drawing conducted at room temperature and at 170 °C using glycerol bath, respectively.

** Fiber effective diameter was determined from SEM cross-sectional images. Tensile testing conducted using gauge length of 25.4 mm and cross-head speed of 1%/s.

*** Crystal size was calculated by Scherrer's equation using (110,200) plane at 2θ ~ 17°. f_{PAN} is Herman's orientation factor of PAN crystals.

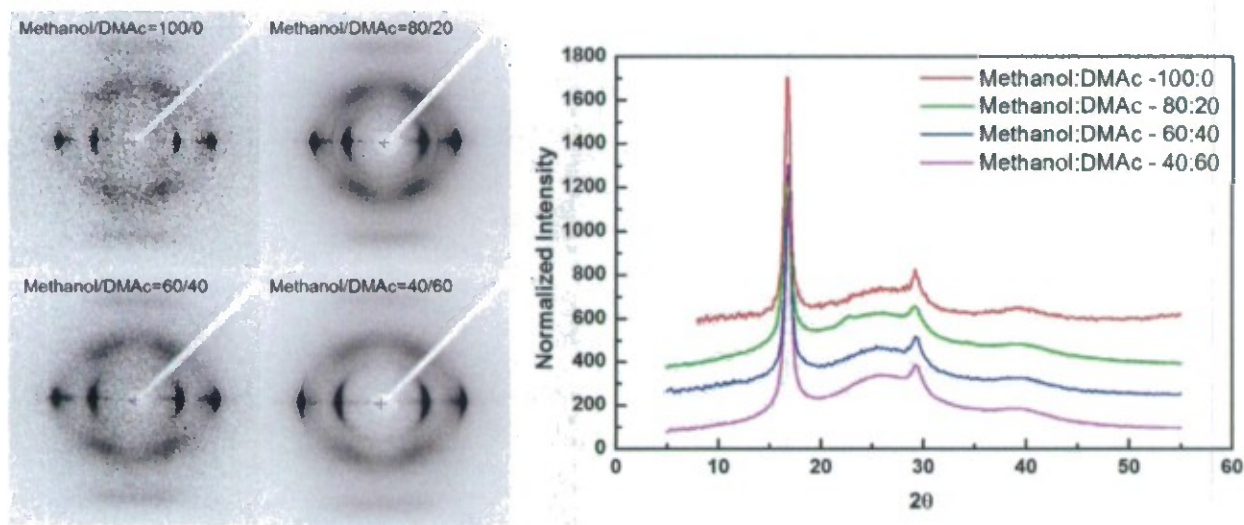


Figure 5. WAXD 2D patterns and integrated scans of various precursor fibers.

4.4 Bi-component (sheath-core) fiber spinning – effect of solution concentration on the resulting fiber properties and effect of gelation bath temperature on the circularity of precursor fiber

In order to process high quality precursor fiber, optimal solution concentration is another key factor. In addition, we tried to vary the gelation bath composition (solvent/non-solvent) for circular fiber as discussed in previous section. Temperature can also be one factor to control the diffusion rate of solvent and non-solvent. In this spinning trial, we tried to vary solution concentration along with varying gelation bath temperature. Processing conditions and fiber properties are listed in Table 5.

Table 5. Processing conditions and properties of various bi-component precursor fibers with varying solution concentration.

	BCFe1	BCFe2	BCFe3	BCFe4	BCFe5	BCFe6	BCFe7
Polymer/solvent	P8 / DMAc						
Concentration (g/dL)	10	11	11.5	11.5	12	12	11
CNT (concentration)	CNTs were not used in these trials						SPO300 (1 wt%)
Solution prep. method	Method 1						
Gelation bath composition	100% methanol						
Gelation bath temperature (°C)	-50	-50	20	-50	20	-50	-50
Spin draw ratio	3	3	2.5	2.5	2.5	2.5	3
Cold draw ratio*	1.3	1.3	1.3	1.3	1.3	1.3	1.25
Hot draw ratio*	4.7	5.7	5.4	5.1	6.7	5.7	5.6
Total draw ratio	18.3	22.2	17.6	16.6	21.8	18.5	21.0
Effective fiber diameter (μm)	8.1	10.4	9.7	9.8	8.2	8.9	6.9
Tensile strength (GPa)**	0.7 ± 0.1	0.6 ± 0.1	0.9 ± 0.1	0.7 ± 0.1	1.0 ± 0.1	0.9 ± 0.1	1.0 ± 0.2
Tensile modulus (GPa)**	21.5±1.0	19.1±1.0	27.3±3.8	23.3±4.0	26.4±1.3	25.3±1.6	23.8±2.8
Strain to failure (%)**	5.5 ± 0.2	5.5 ± 0.2	5.4 ± 0.4	5.3 ± 0.4	6.3 ± 0.3	5.8 ± 0.5	6.9 ± 0.7
Crystallinity (%)	53	52	57	54	56	55	52
Crystal size (nm)	13.3	10.9	13.2	12.6	12.9	12.8	12.5
f_{PAN}^{***}	0.87	0.84	0.92	0.89	0.91	0.91	0.88

* Cold drawing conducted at room temperature. During cold drawing, sheath component (PMMA) was removed using nitromethane. After cold drawing, fiber spool was placed in nitromethane bath for about 2 hr to completely remove sheath component. Hot drawing conducted at 170 °C using glycerol bath.

** Tensile testing conducted using gauge length of 25.4 mm and cross-head speed of 1%/s.

- Effect of solution concentration

As listed in Table 5 (BCFe1, BCFe2, BCFe4, and BCFe6), control PAN fiber was obtained at different solution concentration. Among the fibers, BCFe6 showed the best tensile and structural properties.

- Effect of gelation bath temperature

In Table 5, BCFc3 and BCFc5 fibers were processed at room temperature gelation bath. For comparison, the fibers processed using -50°C gelation bath are also listed (BCFc4 and BCFc6). It can be noted that the fibers gelated at room temperature exhibited slightly better drawability as compared to other fibers in this series, resulting in better tensile and structural properties (as high as 1 GPa tensile strength and 26.4 GPa tensile modulus). The bath temperature can affect the cross-sectional shape of the fiber. In this regard, we have also conducted single component gel spinning using different gelation bath temperatures (100% methanol). SEM cross-sectional images of these fibers are shown in Figure 6(a1 and a2). The fibers processed using room temperature bath showed relatively good circularity as compared to -50°C specimen. This can be attributed to the fact that solvent/non-solvent exchange rate is well balanced at room temperature methanol bath so the fibers did not collapse during gelation/coagulation. In the current study, we also tried bi-component spinning using different bath temperatures to confirm the effect of temperature. The cross-sectional images of these fibers are also shown in Figure 6(b through c). Unlike single-component fiber spinning, the sheath-core fibers spun using -50°C bath exhibited relatively circular cross-sections. We also observed that the sheath component was collapsed after spinning using room temperature bath (Figure 6(b2-1)) whereas spinning using -50°C bath gave the relatively good circular shell component (Figure 6(b1-1)). This may be due to the different solvent/non-solvent exchange rate in the shell component (PMMA solution).

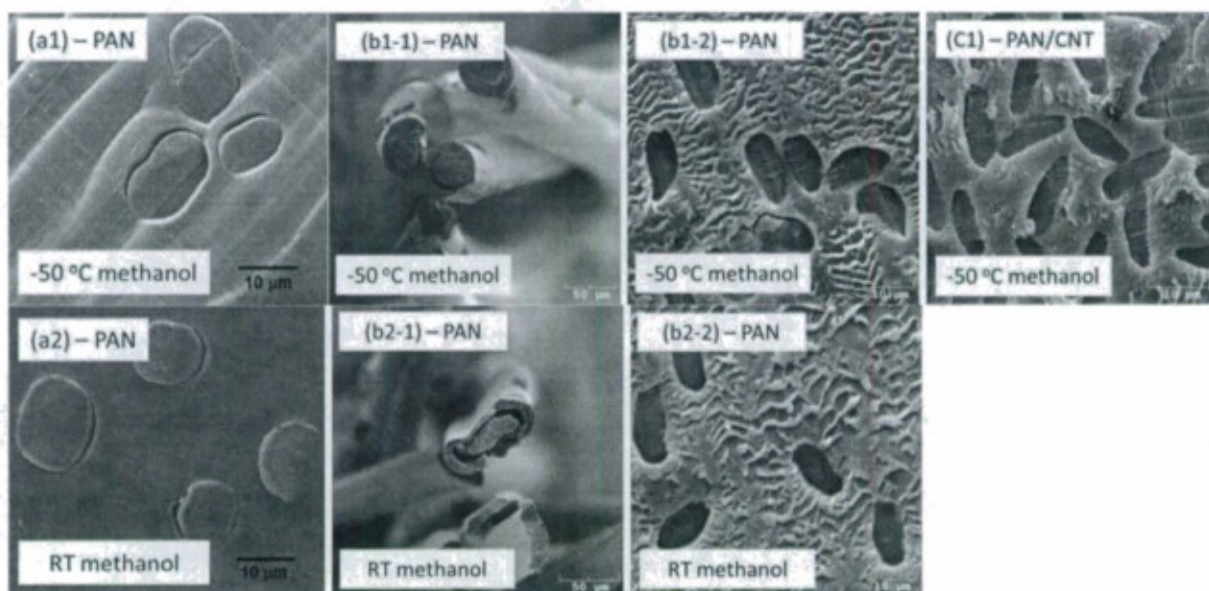


Figure 6. SEM cross-sectional images of (a1 and a2) single component PAN fiber spun using -50°C and RT methanol baths, (b1 and b2) core-shell bi-component PAN fiber spun using -50°C and RT methanol baths, and (c1) core-shell bi-component PAN/CNT fiber spun using -50°C bath, respectively. (b1-1) and (b2-1) are the cross-sectional images of as spun core-shell fiber showing PMMA shell component. (b1-2) and (b2-2) are the cross-sectional images of drawn core-shell fiber after removal of PMMA shell component.

- Effect of carbon nanotube

BCFc7 fiber in Table 5 is PAN/CNT (1 wt%) composite fiber, exhibiting about 1 GPa tensile strength and 24 GPa tensile modulus. These properties are close to the targeted precursor fiber properties (tensile strength > 1 GPa and tensile modulus > 25 GPa). As shown in Figure 5(c1), cross-sectional shape of PAN/CNT composite fibers is collapsed structure more than that of the control PAN fiber, suggesting that solvent removal rate may be faster in PAN/CNT/DMAc solution as compared to that of PAN/DMAc at -50 °C.

4.5 Single component fiber spinning – optimize processing conditions and spinning trial with high molecular weight polymer

- Single component fiber spinning using moderate molecular weight polymer

In previous section, we processed sheath-core bi-component fibers for stabilization and carbonization. However, due to the solution inhomogeneity issue (BCFc7), it was difficult to obtain a precursor fiber that was worth carbonizing. Therefore, an attempt was made to use single component fiber spinning to obtain the smallest diameter precursor fibers with the highest tensile properties using moderate molecular weight (240,000 g/mol) poly(acrylonitrile-co-methacrylic acid) (PAN-co-MAA). Processing conditions and precursor fiber properties are listed in Table 6. All the precursor fibers exhibited high tensile strength (> 1 GPa) and high modulus (> 25 GPa).

Table 6. Processing conditions and properties of various single component precursor fibers with moderate molecular weight.

	SCF8	SCF9	SCF10
Polymer/solvent/concentration	P4 / DMAc / 14 g/dL		
CNT (concentration)	XO122UA (0.5 wt%)		
Solution prep. method	Method 1		
Gelation bath temperature	-50 °C		
Spin draw ratio	3	3	6
Cold draw ratio	2.3	1.8	1.4
Hot draw ratio*	5.5	7.3	4.5
Total draw ratio	38	39	38
Effective fiber diameter (μm)	14.5	13.5	10.1
Tensile strength (GPa)**	1.1 ± 0.1	1.2 ± 0.1	1.0 ± 0.1
Tensile modulus (GPa)**	28.5 ± 0.9	27.3 ± 1.5	25.7 ± 1.9
Strain to failure (%)**	7.0 ± 0.6	7.1 ± 0.5	7.0 ± 0.5

- Single component fiber spinning using high molecular weight polymer
High molecular weight PAN-co-MAA copolymer (P7) with 0.5 wt% CNT (few-wall carbon nanotube, XO122UA) was used for this spinning trial. Processing conditions and resulting precursor fiber properties are listed in Table 7. Overall tensile properties are lower than those of fiber prepared using moderate molecular weight PAN-co-MAA (240,000 g/mol). The solution with 750,000 g/mole polymer exhibited greater degree of inhomogeneity than the solution from 240,000 g/mole polymer, resulting in lower mechanical properties.

Table 7. Processing conditions and properties of various single component precursor fibers with high molecular weight.

	SCF12	SCF12	SCF13
Polymer/solvent/concentration	P7 / DMAc / 7 g/dL		
CNT (concentration)	XO122UA (0.5 wt%)		
Solution prep. method	Method 1		
Gelation bath temperature	-50 °C		
Spin draw ratio	3	6*	6*
Cold draw ratio	1.5	1.5	1.5
Hot draw ratio*	4.8	3.1	3.9
Total draw ratio	21.6	27.9	35.1
Effective fiber diameter (μm)	10.2	13.9	11.4
Tensile strength (GPa)	0.8 ± 0.1	0.7 ± 0.1	0.9 ± 0.1
Tensile modulus (GPa)	17.5 ± 0.8	15.5 ± 0.8	17.2 ± 0.4
Strain to failure (%)	7.8 ± 0.5	9.2 ± 1.2	8.1 ± 0.6

* Prior to cold drawing for 6 day gelation sample, we tried to soak the fiber both in methanol bath and in water+glycerol (50:50) mixture for about 2 – 3 hr in order to assess the effect of bath on the drawability of fiber. The as-spun fiber soaked in water+glycerol mixture exhibited higher drawability and resulted in higher tensile properties.

4.6 Bi-component (sheath-core) fiber spinning – optimize processing conditions for small diameter precursor fiber

In order to obtain small diameter precursor fiber, sheath-core bi-component spinning conducted for this trial. Processing conditions and resulting fiber properties are listed in Table 8.

Table 8. Processing conditions and properties of precursor fibers processed by sheath-core geometry.

	BCFc8	BCFc9
Polymer/solvent/concentration	P1 / DMF / 14.5g/dL	
CNT (concentration)	XO122UA (0.75 wt%)	
Solution prep. method	Method 1	
Gelation bath temperature	-50 °C	
Flow rate (sheath/core) (cc/min)	0.7 / 0.3	
Spin draw ratio	3	3
Cold draw ratio	1.36	1.19
Hot draw ratio	5.0	7.06
Total draw ratio	20.4	25.2
Effective fiber diameter (μm)	7.9	6.9
Tensile strength (GPa)	0.89 ± 0.09	1.11 ± 0.09
Tensile modulus (GPa)	21.5 ± 2.0	21.9 ± 1.5
Strain to failure (%)	7.6 ± 1.0	9.7 ± 1.0
Crystallinity (%)	64	66
Crystal size (nm)	10.0	10.3
f_{PAN}	0.90	0.91
f_{CNT}	0.91	0.93

Tensile strength and modulus of BCFc9 fiber were as high as 1.3 and 24 GPa, respectively, while average tensile strength and modulus was 1.1 and 21.9 GPa. These modulus values are before instrumental compliance correction. Structural analysis (WAXD and Raman spectroscopy) shows that the core precursor fiber has slightly improved structural properties as compared to those of previous core precursor fiber (Table 5). Figure 7 exhibits various characterization results of PAN/CNT core fiber of Table 8. SEM cross-sectional images of precursor fibers are shown in Figure 8. As compared to previous single component spinning trials, the current core PAN/CNT fibers have improved circularity in cross-section.

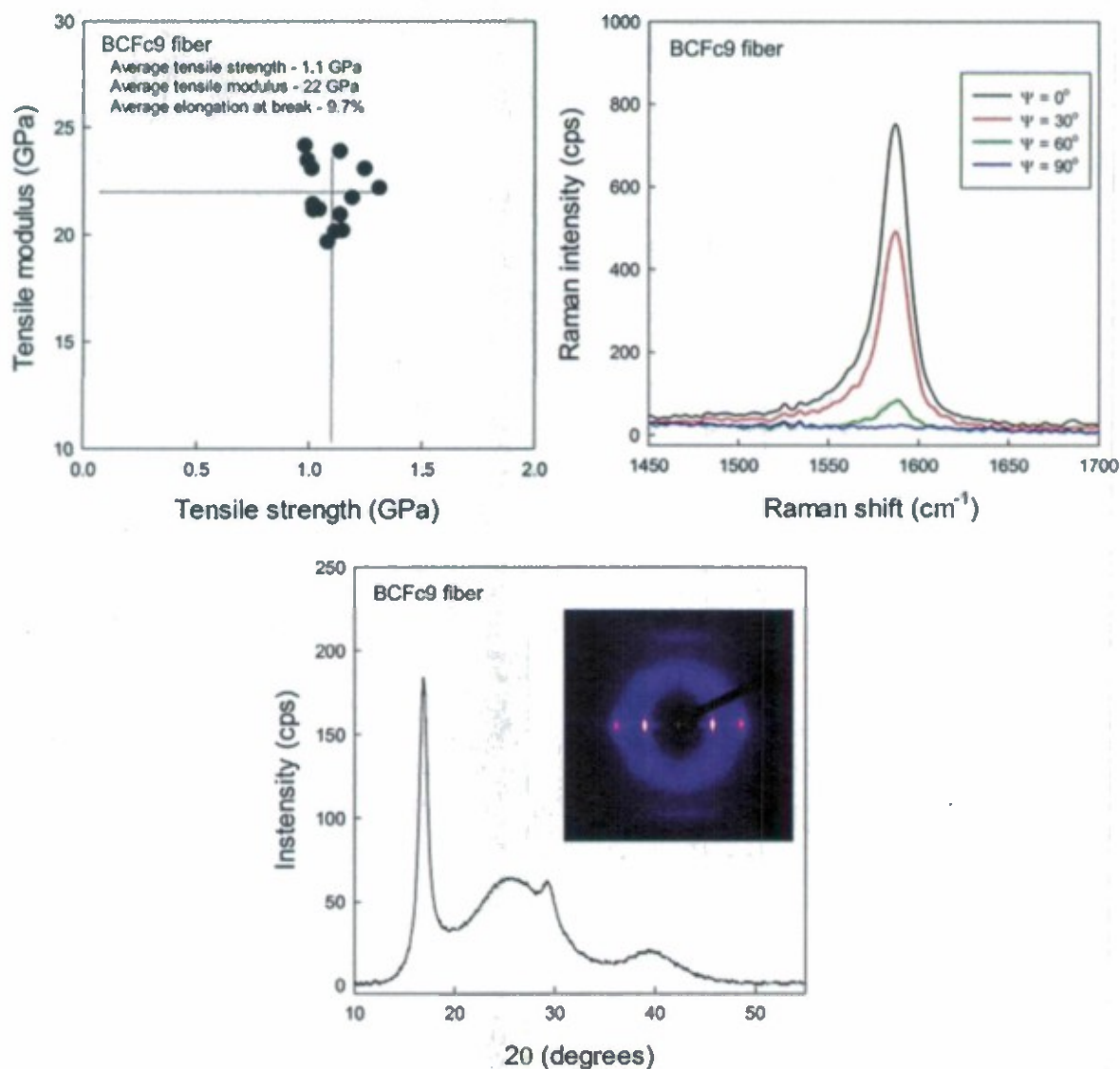


Figure 7. Top left: tensile testing results showing the variation in tensile modulus vs tensile strength, Top right: angular dependence of Raman G-band intensity, Bottom: integrated WAXD scan and 2D diffraction pattern (inset) of BCFc9 precursor fiber.

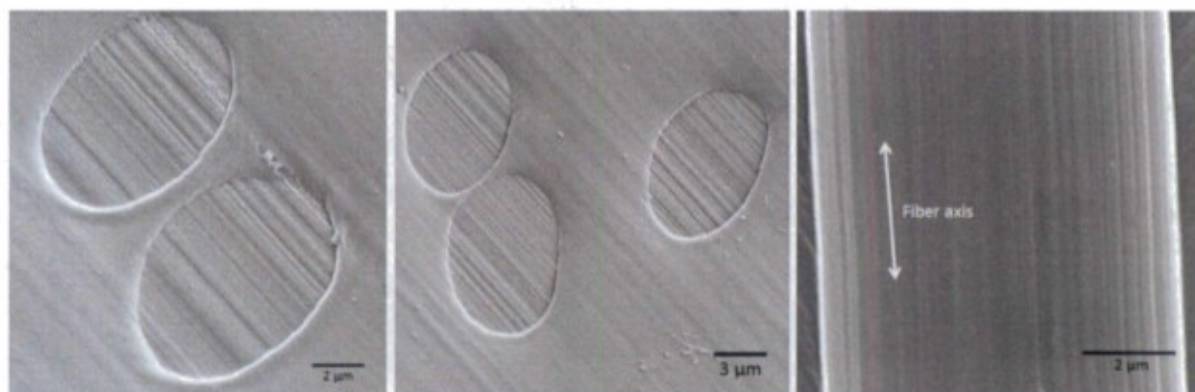


Figure 8. SEM cross-sectional images (left and middle), and surface image (right) of BCFc9 precursor fiber.

4.7 Bi-component (sheath-core) fiber spinning – using various high molecular weight copolymers

Various copolymers with an intermediate molecular weight ($\sim 500,000$ g/mol) were used to process sheath-core bi-component fiber. Processing conditions and precursor fiber properties are listed in Table 9. We obtained less than $7\ \mu\text{m}$ effective fiber diameter for all the spinning/drawing trials. BCFc10 and BCFc11 fibers exhibited relatively lower properties as compared to the previous sheath-core bi-component fibers (Table 8). In addition, during drawing of BCFc12 fibers, cold drawn fibers showed sticking tendency during unwinding due to which the fibers kept breaking during hot drawing. Therefore, enough length of drawn fiber could not be achieved for this sample.

Table 9. Processing conditions and properties of sheath-core precursor fibers from high molecular weight copolymers.

	BCFc10	BCFc10R	BCFc11	BCFc12
Polymer/solvent/concentration	P5 / DMF / 11g/dL		P2/DMF/ 11 g/dL	P6/DMF/ 11 g/dL
CNT (concentration)	XO122UA (1 wt%)			
Solution prep. method	Method 2			
Gelation bath temperature	100% methanol / $-50\ ^\circ\text{C}$			
Flow rate (sheath/core) (cc/min)	0.7 / 0.3			
Spin draw ratio	3	3	3	3
Cold draw ratio	1.2	1.2	1.23	1.23
Hot draw ratio	6.3	6.7	4.9	Fibers stuck together after cold drawing.
Total draw ratio	22.5	24.0	18.2	
Effective fiber diameter (μm)	6.8	6.6	6.6	
Tensile strength (GPa)	0.9 ± 0.1	1.0 ± 0.2	0.8 ± 0.1	
Tensile modulus (GPa)	16.9 ± 1.5	17.9 ± 5.2	19.4 ± 2.4	
Strain to failure (%)	9.2 ± 0.8	8.4 ± 1.2	7.1 ± 0.5	

It is noted that the solution preparation method for these spinning trials was different from previous trials. Although we considered this method (method 2) to be better than method 1 in terms of molecular weight reduction for polymer, the resulting fiber properties indicate that this method may not be good for obtaining homogeneous spinning dope. Carbonization trial (Table 18 and Table 19 in section 5.2) of these precursor fibers also showed lower properties as compared to the carbonization trials conducted with the fibers obtained from solution preparation method 1 (section 4.6 for precursor / Table 15 and Table 16 in section 5.2 for carbonization results).

4.8 Summary and key-outcomes of various spinning trials

- Various spinning trials including single- and bi-component fiber spinning conducted to obtain precursor fiber for carbonization.
- The obtained precursor fiber properties are in the range of
 - Tensile strength: 0.6 – 1.4 GPa
 - Tensile modulus: 16 – 28 GPa
- In order to obtain circular cross-sectional shape of fiber from single component fiber spinning, the higher bath temperature and higher concentration of solvent (DMF or DMAc) in the gelation bath was used successfully. However, in case of bi-component spinning, the solidification process seems to be different from that of single component fiber. Under the similar gelation condition (lower bath temperature), core fibers from bi-component spinning exhibited more circular fiber than single component fiber. In addition, PAN/CNT composite fiber exhibited more flat cross-section than the control fiber processed at similar condition.

5. Stabilization and Carbonization of various precursor fibers

In this section, various efforts for optimizing stabilization and carbonization conditions are presented.

5.1 Stabilization and carbonization for single component PAN/CNT composite fiber

- **Carbonization trials with precursor SCF3**

Stabilization was conducted at various conditions as listed in Table 10. The resulting carbon fiber diameter was determined using SEM cross-sectional images. Without significant processing optimization, 4.3 GPa tensile strength and 406 GPa tensile modulus was obtained for this carbon fiber. Figure 9 shows the tensile test data of carbonized SCF3 for all three carbonization trials and SEM fractured surface images of carbonized SCF3.

Table 10. Processing conditions and resulting carbon fiber properties based on SCF3.

Trial*		1 st	2 nd	3 rd
Residence time (min)	1 st stabilization (at 255 °C)	60		
	2 nd stabilization (at 320 °C)	27.5	17.5	7.5
Carbonization		1100 °C for 5 min		
Effective fiber diameter (μm)		4.3		
Tensile strength (GPa)**		3.5 ± 0.6	4.3 ± 1.0	3.6 ± 0.4
Tensile modulus (GPa)**		378 ± 28	406 ± 28	400 ± 28
Strain to failure (%)**		0.96 ± 0.14	1.05 ± 0.18	0.92 ± 0.10

* For all trials, 36 MPa of pretension was applied to fiber bundle.

** Tensile testing conducted using gauge length of 6 mm and cross-head speed of 0.1%/s.

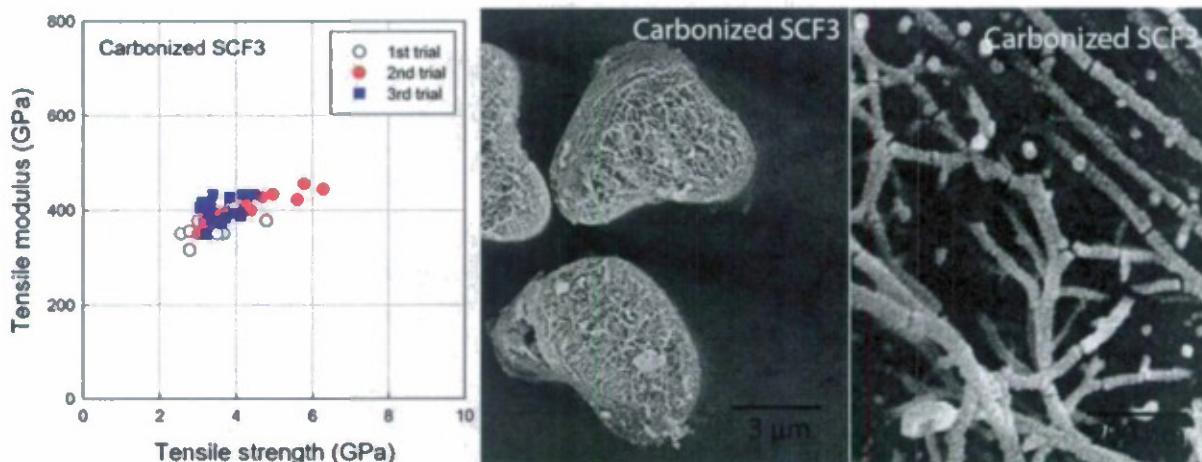


Figure 9. Tensile modulus vs tensile strength of carbonized SCF3, and SEM images of fractured surface of carbonized SCF3.

- **Carbonization trials with precursor fibers prepared during Phase I study**

While optimizing the processing conditions for precursor fibers, carbonization experiment continued on the previously processed (in Phase I study) single component PAN/CNT precursor fiber. Precursor fiber properties are listed in Table 11. Various stabilization and carbonization conditions are also listed in Table 12. The resulting carbon fiber diameter was determined using SEM cross-sectional images. Average tensile strength and modulus values of 4.6 GPa and 303 GPa were obtained with a relatively large carbon fiber diameter, respectively. Figure 10 shows SEM cross-sectional images of carbon fibers from this trial.

Table 11. Properties of precursor PAN/CNT fiber.

	Diameter (μm)	Tensile strength (GPa)	Tensile modulus (GPa)	Strain to failure (%)	Crystallinity (%)	Crystal size (nm)	f_{PAN}
PAN/CNT	11.2	0.85 ± 0.06	20.7 ± 1.4	6.9 ± 0.3	51	8.7	0.883

*P4 polymer (PAN-co-MAA copolymer with $M_v \sim 240,000$ g/mol) and XO122UA CNT (1 wt%) were used for precursor processing.

Table 12. Processing conditions and resulting carbon fiber properties.

Trial*		1 st	2 nd	3 rd	4 th
Residence time (min)	1 st stabilization (at 240 °C)	15	25	35	25
	2 nd stabilization (at 320 °C)	Ramp to 320 °C at 5 °C/min (no holding at 320 °C) and gas change for carbonization			
Carbonization		1100 °C for 5 min			1300 °C for 5 min
Effective fiber diameter (μm)		6.6			5.7
Tensile strength (GPa)**		3.1 ± 0.6	3.7 ± 0.6	3.1 ± 0.4	4.6 ± 0.4
Tensile modulus (GPa)**		217 ± 21	251 ± 23	238 ± 16	303 ± 25
Strain to failure (%)**		1.42 ± 0.22	1.51 ± 0.24	1.31 ± 0.20	1.49 ± 0.12

* For all trials, pretension (53 MPa) was applied to fiber bundle.

** Tensile testing conducted using gauge length of 6 mm and cross-head speed of 0.1%/s.

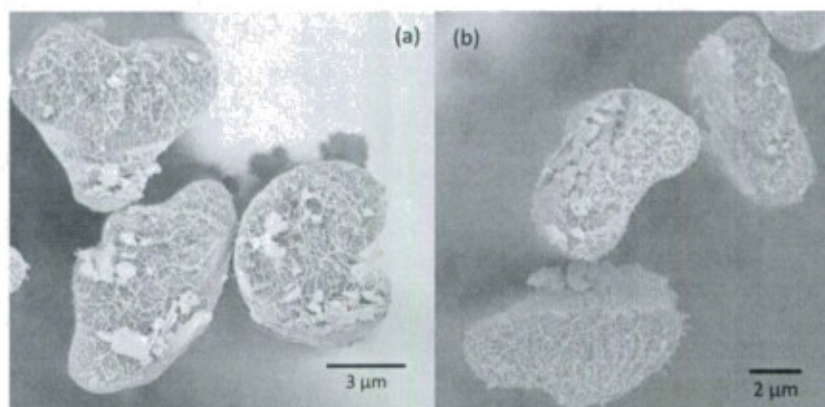


Figure 10. SEM cross-sectional images of carbonized PAN/CNT fiber at (a) 1100 °C and (b) 1300 °C (2nd and 4th trial in Table 12).

- **Carbonization trials with precursor SCF9 and SCF10 – optimal tension for stabilization and carbonization**

In order to determine maximum tension that can be applied to the precursor fiber during stabilization, thermomechanical analysis (TMA) experiments were conducted on SCF9 and SCF10 specimens. In this experiment, fiber strain was observed while heating the fiber up to 380 °C at the constant heating rate of 5 °C/min. As shown in Figure 11, the maximum tension for SCF10 (47 MPa) was slightly higher than that of SCF9 (43 MPa). However, the final strain of SCF9 was close to 20%, which is much higher than that of SCF10 (7%). We found fiber breakage above these tension values.

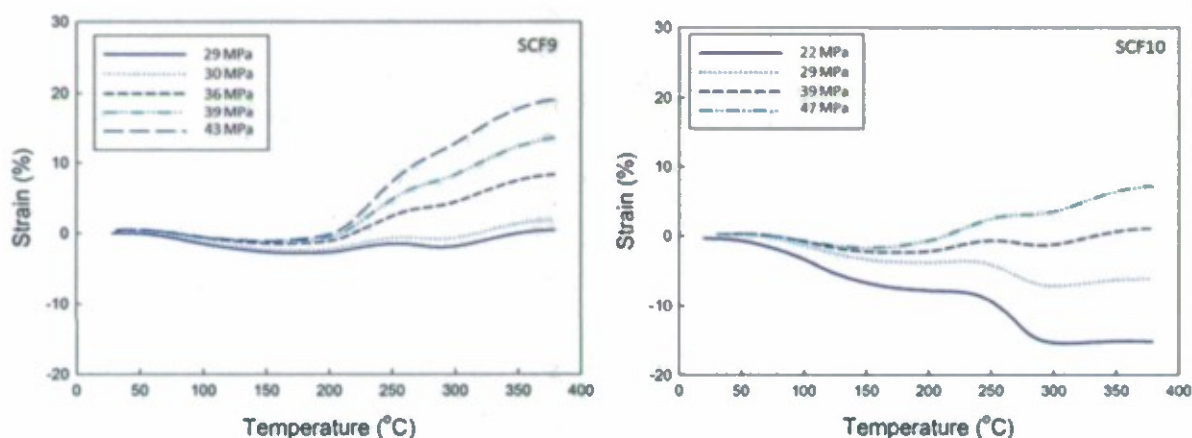


Figure 11. TMA strain curves of precursor fibers (SCF9 and SCF10). Positive and negative strain indicates that fibers stretched and shrunk, respectively.

Stabilization in air was followed by carbonization at various conditions as listed in Table 13. The tensile properties of carbonized SCF9 fiber were significantly higher than those of carbonized SCF10 fiber. The average tensile strength and modulus values were 4.4 GPa and 316 GPa, respectively. However, it should be noted that the stabilization condition was not optimized for both the precursor fibers. In addition, the carbon fiber diameter of this study is in the range of 5 – 6 μm . Figure 12 is the SEM image of carbon fiber surface, showing little or no surface defects. Figure 10 also shows the fractured surface of carbonized fibers. As indicated in the precursor fiber preparation section, these fibers contain only 0.5 wt% of CNT with respect to the polymer matrix. The fractured surface (Figure 12, bottom right) exhibits high volume fraction of nano-fibrils, suggesting good development of CNT templated nano-fibrils.

Table 13. Processing conditions for stabilization and carbonization*, and tensile properties of carbonized fibers.

Sample ID	Trial	Residence time (min)		Effective diameter (μm)	Tensile strength** (GPa)	Tensile modulus** (GPa)	Strain to failure** (%)
		at 265 °C	at 300 °C				
SCF10***	1 st	100 min	30 min	5.7	2.4 ± 0.3	273 ± 24	1.0 ± 0.1
	2 nd	90 min	30 min		2.1 ± 0.4	293 ± 18	1.1 ± 0.3
	3 rd		20 min		3.1 ± 0.4	290 ± 22	1.1 ± 0.1
	4 th		10 min		2.9 ± 0.3	303 ± 24	1.1 ± 0.1
SCF9***	1 st	110 min	30 min	5.4	4.4 ± 0.6	316 ± 26	1.4 ± 0.1

* Carbonization temperature was 1300 °C. After stabilization, argon gas was purged for at least 30 min, and the furnace was heated up to 1300 °C at the constant heating rate of 5 °C/min. At 1300 °C, temperature was held for 5 min. After the carbonization, the furnace was cooled down to room temperature without control.

** Tensile testing conducted using 6 mm gauge length and cross-head speed of 0.1%/s.

*** Tension for stabilization and carbonization for SCF9 and SCF10 was 43 MPa and 46 MPa, respectively.

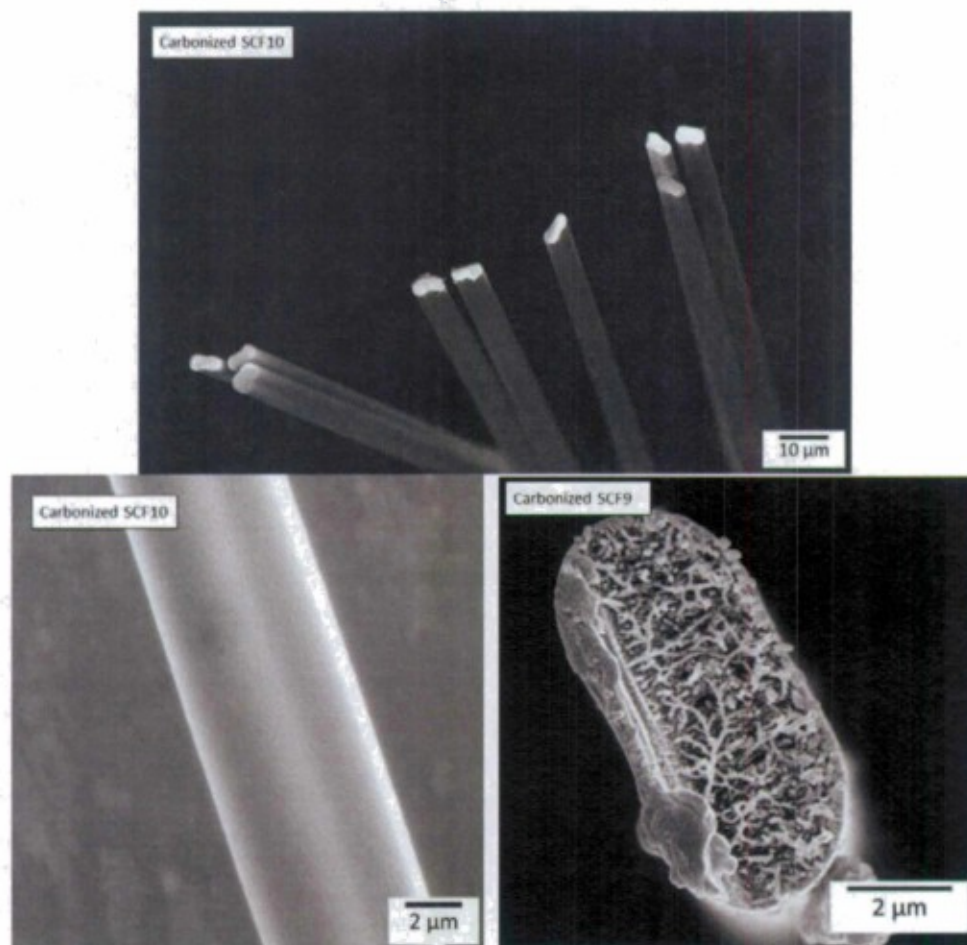


Figure 12. SEM images of carbonized fibers: fractured bundle (top), surface (bottom left), and fractured surface (bottom right). Property data is in Table 13.

Statistical assessment of fracture behavior was carried out using Weibull modulus calculation. Figure 13 shows the plots of linearized Weibull distribution function of commercial carbon fiber (T300) and carbonized SCF9 fiber. As can be seen, the commercial carbon fiber have higher Weibull modulus (11.0) as compared to that of the carbonized SCF9 (8.6) at the same gauge length (6 mm). This shows that the uniformity in the current experimental fiber is not as good as in the commercial fiber, and shows the need for further process refinement.

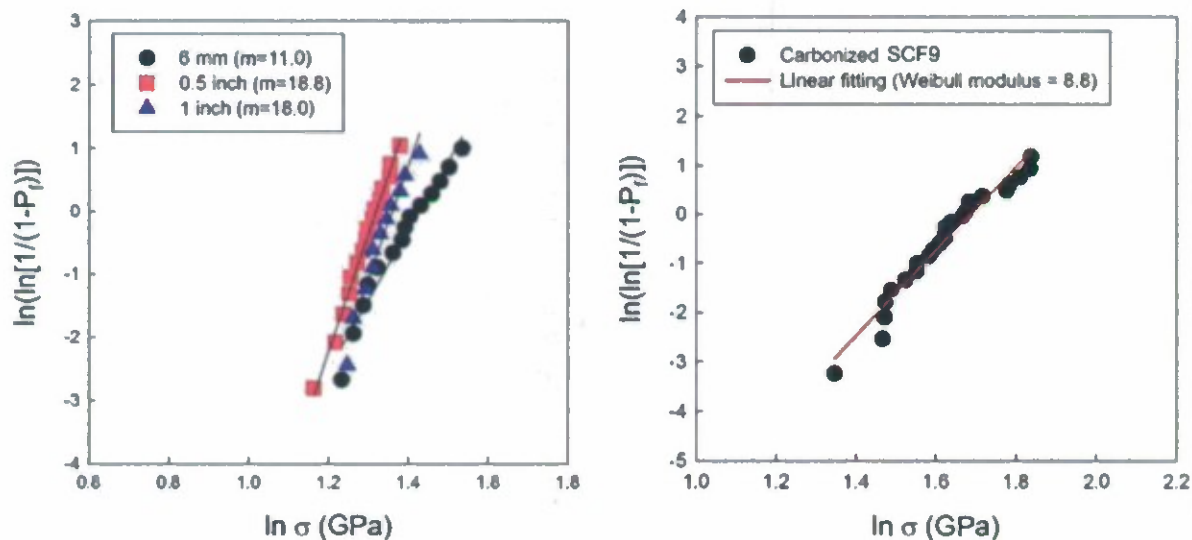


Figure 13. Weibull plot of commercial carbon fiber, T300 (left) and carbonized SCF9 (right).

- **Processing optimization of SCF9 precursor fiber**

Based on above results, SCF9 fiber was used for further processing optimization. The detailed stabilization and carbonization conditions are listed in Table 14. Stabilization in air followed by carbonization in argon environment was conducted at various conditions. Figure 14a and b shows the SEM images of carbon fiber side surfaces, showing very smooth surface with little or no visible surface defects. Figure 14b1 and b2 also show the fractured surface of carbonized fibers. Considering that the precursor fiber contains only 0.5 wt% of CNT, the fractured surfaces exhibit relatively large volume fraction of fibrils. These images confirm not only well dispersed CNTs, but also good development of CNT templated graphitic structure.

The stabilized fiber was carbonized at 1300 °C for 5 min. The best average tensile strength and tensile modulus were about 4.8 GPa and 340 GPa, respectively. Considering the carbon fiber diameter of about 5.4 μm , the current carbon fiber properties are either comparable to the properties of the smaller diameter carbon fiber (effective diameter of about 3 – 4 μm) reported in Phase I study. The fact that tensile strength approaching 5 GPa and tensile modulus approaching 340 GPa can now be obtained for a fiber of 5 μm diameter, represents refinement over previous fiber and is consistent with the relatively defect free images seen in Figure 14. Figure 15 shows the plot of tensile modulus vs tensile strength of various carbon fibers. Compliance correction was done for 6th carbonization trial by testing at various gauge lengths.

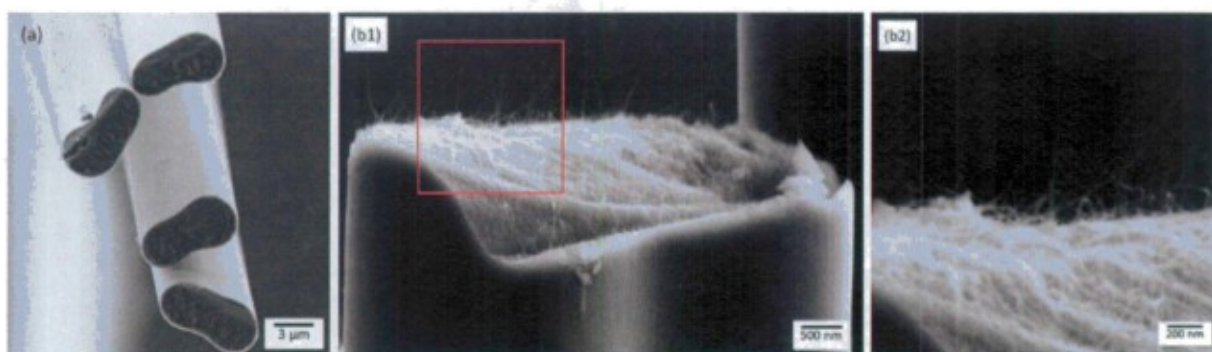


Figure 14. SEM images of carbonized PAN-co-MAA/CNT fiber from SCF9 precursor fiber. (a) and (b) surface and cross-sectional views, (b2) is a high magnification image of square box region of (b1) showing high volume fraction of fibrils.

Table 14. Processing conditions for stabilization and tensile properties of carbonized fibers from precursor SCF9. Pretension for all the trials was 43 MPa based on the precursor fiber diameter. Carbonization conducted at 1300 °C for 5 min.

Trial	Stabilization temp (°C) / residence time (min)		Effective diameter (μm) ^a	Gauge length (mm)	Tensile strength (GPa) ^{****}	Tensile modulus (GPa) ^{****}	Strain to failure (%) ^{****}
	1 st	2 nd					
1 st	265 / 110	300 / 30	5.35	6	4.4±0.6	316±26	1.4±0.1
2 nd	265 / 120	300 / 30		6	4.2±0.9	277±41	1.5±0.2
3 rd	265 / 120	300 / 25		6	4.5±0.6	287±25	1.5±0.2
4 th	265 / 130	300 / 30		6	4.8±0.5	318±24	1.5±0.2
4 ^{th-1**}	265 / 130	300 / 30		6	4.2±0.7	304±24	1.4±0.7
5 ^{th***}	265 / 140	300 / 30		6	3.9±0.5	258±29	1.5±0.1
6 ^{th-1}	265 / 140	300 / 30		6	4.1±0.8	296±37	1.4±0.2
6 ^{th-2}				12.7	3.5±0.6	310±24	1.1±0.1
6 ^{th-3}				25.4	3.1±0.4	316±22	1.0±0.1
7 th	265 / 130	320 / 10		6	4.0±0.6	320±31	1.2±0.2
8 th	265 / 130	320 / 20		6	4.4±1.0	326±40	1.3±0.3
9 th	265 / 130	320 / 30		6	3.5±0.7	337±32	1.0±0.2

* Carbon fiber diameter in the current report is based on SEM calibration.

** 4^{th-1} specimen was same as 4th trial. However, the testing specimen was soaked in detergent (domestic dishwashing detergent, Palmolive antibacterial, 3 wt% detergent and 97% water) for about a week and retested.

*** For 5th trial, tungsten clamp slipped out of the fiber after carbonization while the furnace was being cooled down to room temperature (at about 500 °C).

**** All the carbon fiber tensile testing was done at strain rate of 0.1%/s at different gauge lengths using RSA III. Typically 20 – 30 specimens were tested for each gauge length.

Structural analysis by WAXD and Raman spectroscopy was done for trial 4th sample and the data is shown in Figure 16. WAXD results show the typical diffraction pattern of carbon fiber. However, Raman spectrum suggests that the current carbon fiber (4th trial) possesses highly graphitic structure as confirmed by strong G-band intensity at around 1590 cm⁻¹. This suggests, perhaps higher volume fraction of more perfect graphitic fibrils. Carbon fiber tensile strength data was also analyzed using Weibull statistical analysis. Figure 17 shows the plots of linearized

Weibull distribution function of carbon fibers (1st and 4th trials). For 4th carbonization trial, the calculated Weibull modulus was 12.6, which is higher than 1st carbonization trial (8.6) and even higher than the commercial carbon fiber (T-300, Weibull modulus = 11 in Figure 13) at the same gauge length (6 mm).

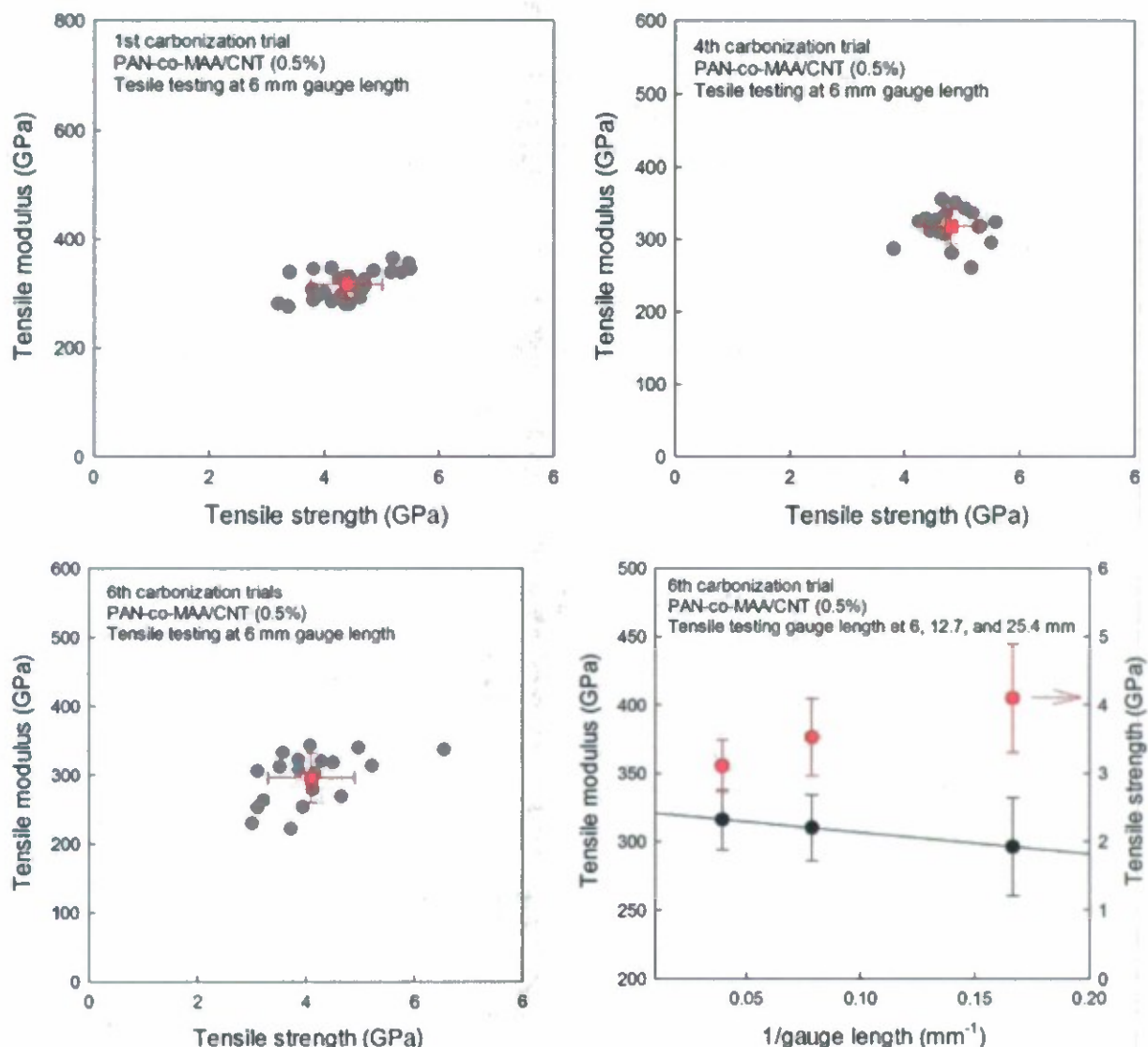


Figure 15. Tensile modulus vs tensile strength of various carbonization trials and gauge length dependence of tensile properties of 6th carbonization trial specimen. Summary data is in Table 14.

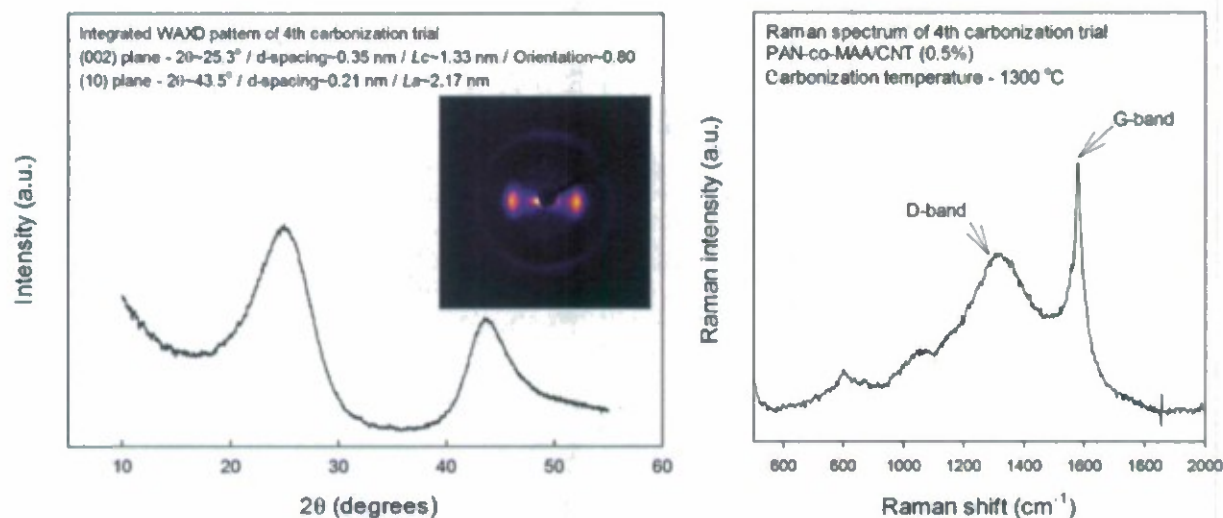


Figure 16. Integrated WAXD pattern and analysis results (left), and Raman spectra of carbonized SCF9 fiber (right). This data is for the 4th carbonization trial.

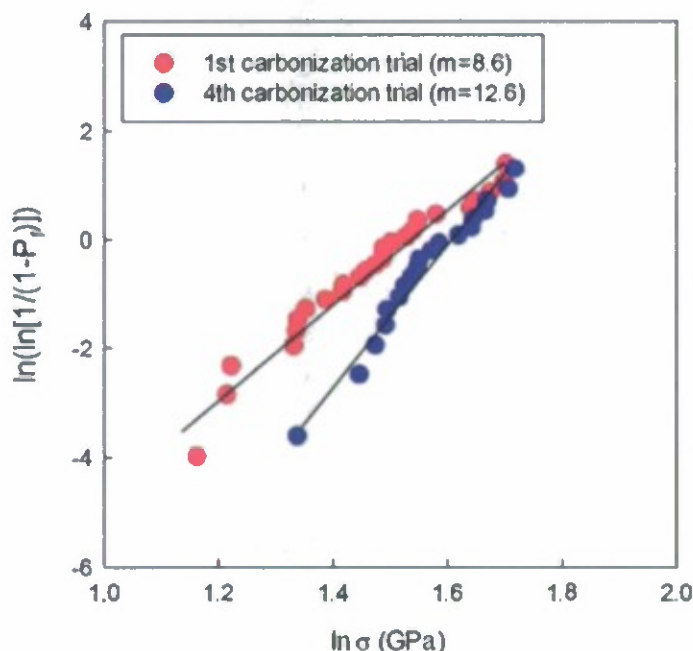


Figure 17. Weibull plot of 1st and 4th carbonization trials.

5.2 Stabilization and carbonization for sheath-core bi-component fiber

- Carbonization trials with BCF₉ precursor fiber and processing optimization

BCF₉ precursor fiber was selected for stabilization and carbonization. In the preliminary stabilization and carbonization experiment, pretension of 25.5 MPa was used and residence time at various temperatures was set as 50 min at 260 °C and 30 min at 305 °C. These conditions were determined based on previous stabilization experiment. However, the tensile strength and modulus of resulting carbon fibers were only as high as about 3.8 GPa and 270 GPa, respectively, as shown in Table 15. The morphological study

on this fiber by SEM (Figure 18) exhibited highly porous structure on the surface of carbon fiber, indicating that the stabilization condition was not appropriate. It was also noted that the fibers shrank during stabilization.

Therefore, different stabilization conditions such as longer stabilization time and higher pretension values were used in subsequent experiments. It should be noted that trial number for carbonization at different conditions begins from trial 6. Trial number 1 to 5 was done by changing the residence time at high temperature in stabilization, but all those 5 trials produced similar property carbon fibers. At similar pretension (at 25.5 MPa), the longer stabilization time (at lower temperature, 260 °C) brought about similar tensile strength, but higher modulus (295 GPa vs 270 GPa). The subsequent carbonization trials were achieved by changing pretensions to 27.3, 29.4, and 34.7 MPa. All the trials were successful, and no filaments were broken during stabilization and carbonization. Figure 18 shows SEM surface and cross-sectional images of carbon fiber from trial 9. As compared to trial 1 fiber, trial 9 fiber does not have noticeable defect (pore) structure, suggesting that the stabilization in trial 9 was done in more optimal conditions than in trial 1. In addition, one can observe that the well-developed fibrillar structure in trial 9 cross-sectional image. The highest tensile strength and modulus were 6.5 GPa and 390 GPa, respectively (Figure 19). Carbon fiber tensile testing was conducted at 6 mm gauge length and compliance corrected modulus is about 400 GPa. Tensile testing results of trial 9 are shown in Figure 19 along with Weibull analysis results of the data reported in Table 15. Trial 9 exhibited the highest Weibull modulus ($m=9$) as compared to the other carbonization trials.

Table 15. Processing conditions and properties of carbonized BCFc9 fiber.

Trial	Pre-tension (MPa)*	Stabilization time		Effective diameter (μm) ‡	Tensile strength (GPa) **	Tensile modulus (GPa) **	Strain to failure (%)**	Weibull modulus
		at 260 °C (min)	at 305 °C (min)					
1 st #	25.5	50	30	3.76	3.83±0.37	271±31	1.41±0.19	5.9
8 th #	25.5	90	10	3.76	3.83±0.61	295±24	1.30±0.22	6.3
7 th #	27.3			3.54	4.22±0.57	315±35	1.33±0.17	7.4
8 th #	29.4			3.52	4.90±0.69	339±24	1.43±0.16	7.0
9 th #	34.7			3.50	5.48±0.58	362±15	1.52±0.15	9.0

* Pretension was applied by graphite clamps and adjusted by changing number of filaments.

‡ Effective diameter was calculated from the SEM cross-sectional images of various fibers. At least 20 different cross-sections were observed and used to calculate cross-sectional area (by ImageJ image analysis software).

** Tensile testing was done at 6 mm gauge length at a constant strain rate of 0.1%/s.

In all the trials, carbonization was done at 1300 °C in an inert environment (argon). The ramping rate was at 5 °C/min and temperature was held at 1300 °C for 5 min.

After carbonization trial 9 with BCFc9 precursor fiber, various experiments were conducted to optimize stabilization conditions by varying tension and residence time during stabilization. In the first stage of experiments (Trial 9-1 to Trial 9-13), we conducted stabilization and carbonization by varying tension to find the maximum tension for processing. As can be seen from Table 16, 34.7 MPa was the highest tension, but the processing stability was very poor. We observed frequent fiber breakage although

few trials were successful. Moreover, the successful trials produced lower properties of carbon fiber as compared to Trial 9. Therefore, we reduced tension to about 33.2 MPa, resulting in much more stable processing.

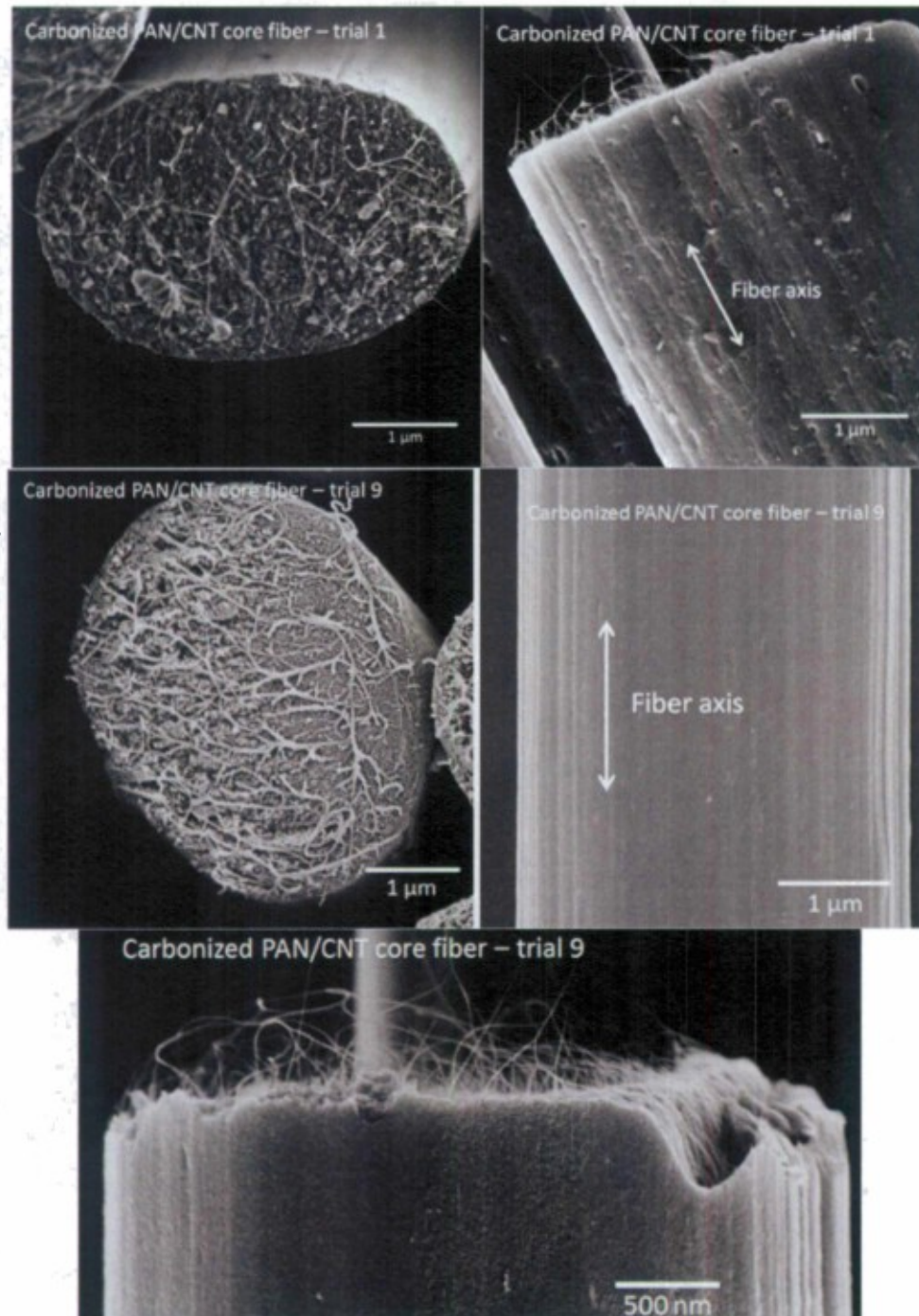


Figure 18. SEM images of carbon fibers (trial 1 and 9 in Table 15) showing cross-sections and surface of carbon fibers. Trial 1 fiber shows pore structure on the surface (as large as 200 – 300 nm), while trial 9 fiber does not show noticeable defect structure. Trial 9 fiber also shows larger fibrillar structure than trial 1, indicating better stabilization conditions.

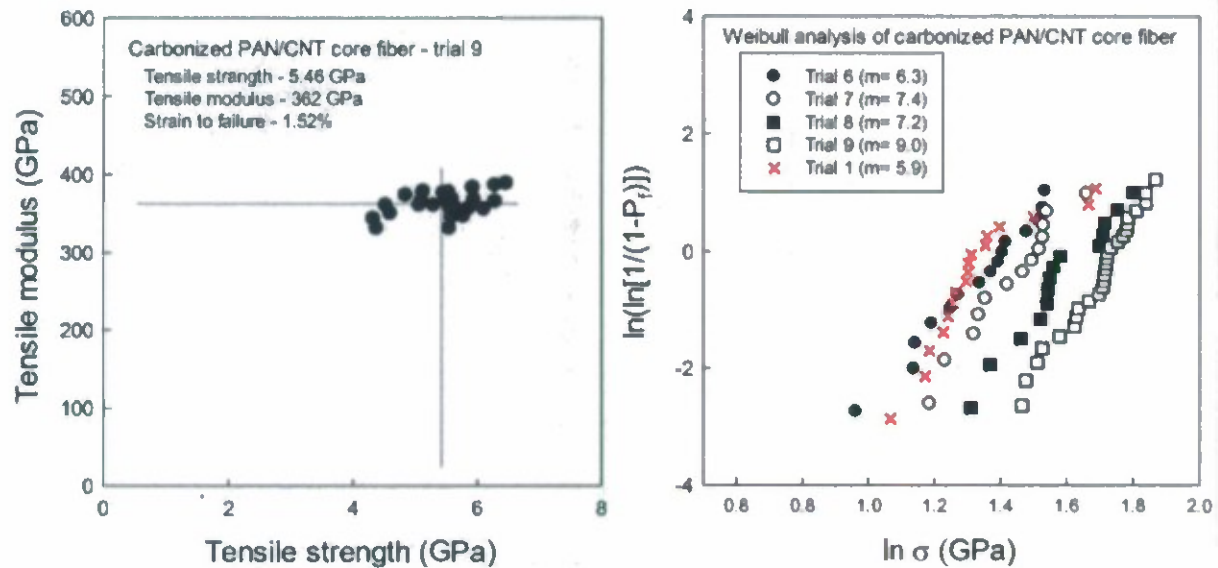


Figure 19. Tensile testing and Weibull analysis results of various trials (in Table 15) are also shown. Carbon fiber tensile testing was done at a gauge length of 6 mm and modulus was not corrected for instrumental compliance.

In order to find the optimal stabilization conditions more effectively, the design of experiments method was adopted for determining various processing parameters. In the second stage of experiment (Trial 10 to Trial 17 in Table 16), a center point of experiment was chosen as 110 min (t_1) at 260 °C and 10 min (t_2) at 305 °C. Then, a range of values for each variable (t_1 and t_2) was determined based solely on the region of interest. These time ranges were 90 – 130 min and 0 – 20 min for t_1 and t_2 , respectively. The carbonization condition was same as the other trials.

Combined with the experimental result, the simple linear model for design of experiment produced the following equation to predict the expected tensile strength.

$$\text{Tensile strength} = -15.16 + 8.57 \cdot 10^{-3} e_1 - 0.28 e_2 + 9.81 e_1^2 + 22.08 e_2^2 + 0.07 e_1 e_2$$

where, e_i can be described as following equation.

$$e_i = (t_i - t_{i,avg})/\alpha$$

where α is a scaling factor (in the current case, it is 1.414) and t_i is either t_1 (residence time at 260 °C) or t_2 (residence time at 305 °C). $t_{i,avg}$ is the average residence time for either t_1 or t_2 .

Table 17 shows the performance of the above response equation and compared the experimental results and predicted tensile strength values. Although the equation does not yield precise tensile strength, the data is useful as evidenced by its ability to reveal critical points, specifically maximum and minimum.

As can be seen from Figure 20, tensile modulus of carbonized PAN/CNT fibers was about 40% higher than that of industrial carbon fiber (T650), and all the carbonization trials brought about more than 300 GPa tensile modulus at 1300 °C carbonization temperature without compliance correction (corrected modulus, 345 GPa). The highest tensile strength and modulus reached to 6.8 GPa and 389 GPa, respectively.

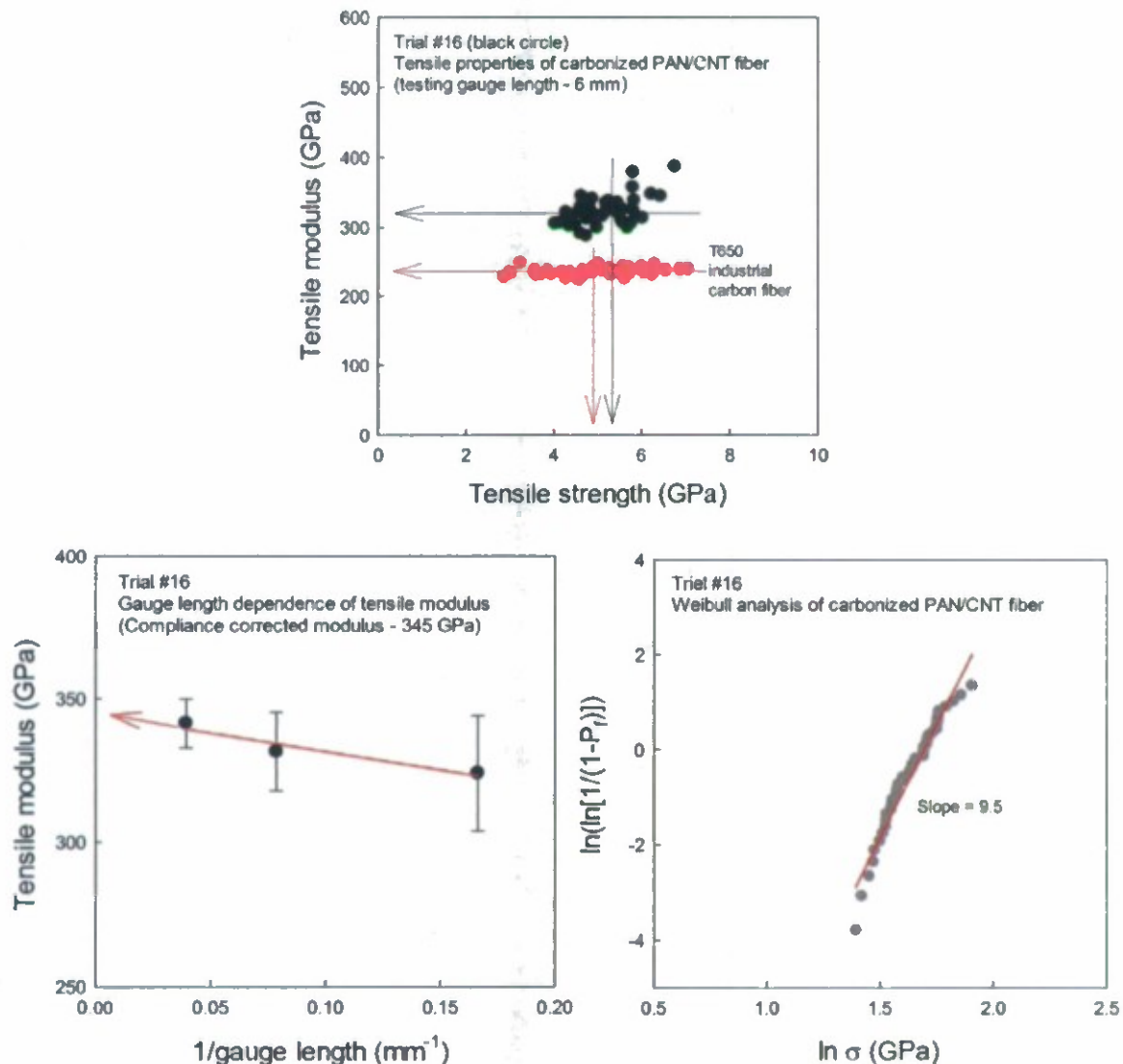


Figure 20. Tensile testing results of carbonized PAN/CNT composite fiber (Trial #16 in Table 16): Tensile modulus vs. tensile strength (top), showing that the highest tensile strength and modulus are up to about 6.8 GPa and 389 GPa, respectively. For comparison, industrial carbon fiber (T650) was also tested at the same testing condition. Tensile modulus of Trial 16 is about 40% higher than that of T650, while tensile strength is slightly higher (about 10%). Gauge length dependence of tensile modulus (bottom left) exhibits that the compliance corrected modulus is about 345 GPa, whereas that of T650 is about 250 GPa (not shown here). Weibull analysis (bottom right) shows the tensile fracture of trial 16 sample is slightly more reliable than that of trial 9 (Weibull modulus = 9.0 in Figure 19).

Table 16. Processing conditions and properties of carbonized PAN/CNT core precursor fiber (BCFc9).

Trial	Pre-tension (MPa)	Stabilization time		Effective diameter† (μm)	Gauge length (mm)	Tensile strength* (GPa)	Tensile modulus* (GPa)	Strain to failure* (%)	Weibull modulus
		at 260 °C (min)	at 305 °C (min)						
9-1	36.4	100	10	• Fiber breakage during stabilization					
9-2	34.7	100	10	• Fiber breakage during stabilization					
9-3	34.7	100	10	3.50	6	3.93 ± 0.85	315 ± 15	1.24 ± 0.27	-
9-4	34.7	100	10	• Fiber breakage during stabilization					
9-5	25.5	100	10	3.50	6	2.20 ± 0.47	238 ± 30	0.91 ± 0.12	-
9-6	30.6	100	10	3.50	6	2.47 ± 0.52	289 ± 24	0.85 ± 0.14	-
9-7	34.7	100	10	• Fiber breakage during carbonization					
9-8	34.7	100	10	3.50	6	4.01 ± 0.57	312 ± 22	1.28 ± 0.19	-
9-9	34.7	90	10	3.50	6	3.87 ± 0.67	346 ± 34	1.11 ± 0.16	-
9-10	34.7	96	3	3.50	6	4.06 ± 0.63	320 ± 15	1.26 ± 0.16	-
9-11	34.7	100	10	• Fiber breakage during stabilization					
9-12	33.2	90	10	3.50	6	3.67 ± 0.56	308 ± 22	1.18 ± 0.24	-
9-13	33.2	100	10	3.50	6	4.40 ± 0.77	319 ± 17	1.37 ± 0.20	-
10	33.2	124	3	3.39	6	4.19 ± 0.43	317 ± 15	1.39 ± 0.14	9.6
11		124	17	3.36		4.03 ± 0.42	323 ± 17	1.29 ± 0.11	10.2
12		96	3	3.41		4.52 ± 0.90	340 ± 25	1.37 ± 0.20	4.9
13		96	17	3.54		4.27 ± 0.74	310 ± 20	1.40 ± 0.18	5.9
14		130	10	3.42		4.84 ± 0.64	316 ± 16	1.55 ± 0.18	8.0
15		90	10	3.40		4.68 ± 0.64	314 ± 20	1.52 ± 0.19	7.7
16		110	0**	3.51	6	5.33 ± 0.55	326 ± 21	1.62 ± 0.15	9.5
					12.7	4.67 ± 0.46	328 ± 11	1.44 ± 0.14	8.8
					25.4	4.41 ± 0.40	341 ± 9	1.28 ± 0.11	11.1
17		110	20	3.42	6	4.26 ± 0.59	325 ± 25	1.34 ± 0.12	7.5

† Linear density (tex) was obtained from vibroscope method and effective diameter was calculated assuming carbon fiber density of 1.8 g/cm³.

* Tensile testing was done at 6, 12.7, and 25.4 mm gauge length as indicated at a constant strain rate of 0.1%/s.

** For trial 16, the second stage of stabilization was done by heating up to 305 °C at a heating rate of 5 °C/min, and then proceed for carbonization without holding at 305 °C.

Table 17. Performance of the response equation based on design of experiment and comparison with the observed tensile strength data.

		Trial 10	Trial 11	Trial 12	Trial 13	Trial 14	Trial 15	Trial 16	Trial 17
t_1	Coefficient	1	1	-1	-1	1.41	-1.41	0	0
	Time (min)	124	127	96	96	130	90	110	110
t_2	Coefficient	-0.66	0.66	-0.66	0.66	0	0	-0.94	0.94
	time (min)	3	17	3	17	10	10	0	20
Predicted (GPa)		4.22	3.94	4.29	3.83	4.48	4.45	4.73	4.19
Observed (GPa)		4.19	4.03	4.52	4.27	4.84	4.68	5.33	4.26

- **Carbonization trials with BCFc10R and BCFc11 precursor fibers and processing optimization**

After completing the various carbonization trials from BCFc9 fiber, we obtained different precursor fibers from high molecular weight polymer (BCFc10R and BCFc11). As discussed, these fibers were prepared from PAN or PAN-co-MAA polymers with an high molecular weight (~500,000 g/mol). We also used different solution preparation method to achieve better homogeneity in spinning dope. However, the precursor fiber properties exhibited that this processing step is somewhat adverse for the precursor fibers. As can be seen from below carbonization results, all the trials did not produce tensile strength more than 3.5 GPa.

Table 18 and Table 19 show the various carbonization trials with BCFc10R and BCFc11. Firstly, we tried to find the maximum tension that the fibers can bear during stabilization and carbonization. Then, the residence time during stabilization was varied to obtain the highest tensile properties. The carbonization condition was same as that for BCFc9 fiber.

Table 18. Processing conditions and properties of carbonized PAN/CNT core precursor fiber (BCFc10R).

Trial	Pre-tension (MPa)	Stabilization time (min)		Effective diameter (μm)	Tensile strength (GPa)	Tensile modulus (GPa)	Strain to failure (%)	Weibull modulus
		260 °C	305 °C					
1	35.6	46	3	3.74	2.6 \pm 0.6	292 \pm 12	0.93 \pm 0.20	1.48
2	39.2	46	3		N/A			
3	43.5	46	3	4.21	3.0 \pm 0.7	279 \pm 17	1.08 \pm 0.28	4.20
4	46.1	35	35	3.60	3.1 \pm 0.6	281 \pm 28	1.11 \pm 0.19	4.72
5		46	17	3.42	2.4 \pm 0.9	292 \pm 20	0.86 \pm 0.31	2.22
6		74	3	3.77	3.1 \pm 1.3	287 \pm 17	1.11 \pm 0.43	1.77
7		74	17	3.38	2.6 \pm 0.4	274 \pm 17	0.97 \pm 0.18	5.27
8	45.8	40	10	3.68	3.4 \pm 0.7	267 \pm 27	1.25 \pm 0.23	4.84
9		80	10	3.50	3.1 \pm 0.9	293 \pm 19	1.10 \pm 0.27	3.35
10		60	0	3.56	3.3 \pm 0.5	299 \pm 13	1.12 \pm 0.15	6.95
11		60	10	3.56	2.6 \pm 0.5	299 \pm 12	0.92 \pm 0.16	2.62
12		60	20	3.43	3.2 \pm 0.7	287 \pm 12	1.13 \pm 0.23	4.77

Table 19. Processing conditions and properties of carbonized PAN/CNT core precursor fiber (BCFe11).

Trial	Pre-tension (MPa)	Stabilization time (min)		Effective diameter (μm)	Tensile strength (GPa)	Tensile modulus (GPa)	Strain to failure (%)	Weibull modulus
		260 °C	305 °C					
2	41.6	Fiber broke during stabilization						
2	33.3	Fiber broke during stabilization						
3	29.7	76	3	3.45	2.7±0.6	275±9	0.99±0.22	3.90
4		76	17	3.36	2.9±0.4	259±8	1.12±0.15	3.16
5		70	10	3.73	2.9±0.4	272±14	1.09±0.13	5.71
6		104	3	3.75	2.6±0.4	277±17	0.95±0.16	6.01
7		104	17	3.34	2.4±0.5	253±18	0.94±0.21	4.49

6. Summary and key-outcomes

- Various carbonization trials were conducted using single- and bi- (sheath-core) component precursor fibers.
- Processing optimization was carried out by varying stabilization conditions such as tension, temperature and residence time.
- The highest average tensile properties from single component ($\sim 10 \mu\text{m}$) precursor fibers are as follows (Table 14 and Figure 14).
 - Tensile strength: 4.8 GPa (the highest tensile strength for a single test 6.5 GPa)
 - Tensile modulus: 337 GPa (the highest tensile modulus for a single test 360 GPa)
- The highest average tensile properties from bi-component ($\sim 7 \mu\text{m}$) precursor fibers are as follows (Table 15 and Figure 19).
 - Tensile strength: 5.5 GPa (the highest tensile strength for a single test 6.8 GPa)
 - Tensile modulus: 362 GPa (the highest tensile modulus for a single test 389 GPa)